Protein Science (1996), 5:5–12. Cambridge University Press. Printed in the USA.

Identification of an essential acidic residue in Cdc25 protein phosphatase and a general three-dimensional model for a core region in protein phosphatases

JENS W. ECKSTEIN, PEGGY BEER-ROMERO, AND INGRID BERDO

Mitotix, Inc., One Kendall Square, Cambridge, Massachusetts 02139

(RECEIVED July 27, 1995; ACCEPTED October 12, 1995)

Abstract

The reaction mechanism of protein tyrosine phosphatases (PTPases) and dual-specificity protein phosphatases is thought to involve a catalytic aspartic acid residue. This residue was recently identified by site-directed mutagenesis in *Yersinia* PTPase, VHR protein phosphatase, and bovine low molecular weight protein phosphatase. Herein we identify aspartic acid 383 as a potential candidate for the catalytic acid in human Cdc25A protein phosphatase, using sequence alignment, structural information, and site-directed mutagenesis. The D383N mutant enzyme exhibits a 150-fold reduction in k_{cat}, with K_m only slightly changed. Analysis of sequence homologies between several members of the Cdc25 family and deletion mutagenesis substantiate the concept of a two-domain structure for Cdc25, with a regulatory N-terminal and a catalytic C-terminal domain. Based on the alignment of catalytic residues and secondary structure elements, we present a three-dimensional model for the core region of Cdc25. By comparing this three-dimensional model to the crystal structures of PTP1b, *Yersinia* PTPase, and bovine low molecular weight PTPase, which share only very limited amino acid sequence similarities, we identify a general architecture of the protein phosphatase core region, encompassing the active site loop motif HCXXXXXR and the catalytic aspartic acid residue.

Keywords: catalytic acid; homology modeling; human Cdc25 protein phosphatase; protein phosphatases

Protein tyrosine phosphatases (PTPases) and dual-specificity protein phosphatases are growing families of enzymes involved in the regulation of a variety of cellular events (for reviews see Fischer et al., 1991; Stone & Dixon, 1994). Their role in fundamental processes such as signal transduction and cell-cycle regulation is the subject of a variety of studies aimed at understanding the substrate specificity and regulation of these enzymes.

Protein phosphatases share the common active site motif **(H)CXXXXXR**, which includes a nucleophilic cysteinyl residue and defines the binding site for the tyrosyl phosphate substrate (Guan & Dixon, 1990; Pot & Dixon, 1992; Streuli et al., 1990). The pK_a of this cysteine is very low (<5) compared to that of the free amino acid (approximately 8.5) (Zhang et al., 1994c). The cysteine thiolate is thought to attack the electrophilic phosphorus of the phosphotyrosyl residue in the substrate, causing the phosphoester bond to break. The unphosphorylated substrate is then expelled upon protonation (Denu et al., 1995). A covalent thiophosphate ester intermediate between the catalytic nucleophilic cysteine in *Yersinia* PTPase and a ^{32}P-labeled phosphate has been identified (Cho et al., 1992; Guan & Dixon, 1990). Hydrolysis subsequently releases the free phosphate.

Study of the chemical mechanism has implicated a catalytic acid, which is thought to affect the protonation of the dephosphorylated substrate and thus to make it a better leaving group. Dixon and co-workers identified this catalytic acid in *Yersinia* PTPase and VHR by site-directed mutagenesis (Zhang et al., 1994c; Denu et al., 1995). Recently, the crystal structures of the two PTPases PTP1b and *Yersinia* PTPase were reported (Barford et al., 1994; Stuckey et al., 1994). Saper and his group crystallized two forms of *Yersinia* PTPase, one unliganded, the other bearing sulfate in the phosphate binding site. They propose that ligand binding triggers a conformational change that traps the oxyanion and swings Asp 356, the catalytic residue identified by site-directed mutagenesis, by 8 Å into the active site (Schubert et al., 1995).

Cdc25, a dual-specificity protein phosphatase, plays an important role in cell cycle regulation (Russell & Nurse, 1986; Mil-

Reprint requests to: Jens W. Eckstein, Mitotix, Inc., One Kendall Square, Cambridge, Massachusetts 02139.

Abbreviations: PTPase, protein tyrosine phosphatase; LMW-PPase, low molecular weight protein phosphatase; mFP, 3-*O*-methylfluorescein phosphate; pNPP, *p*-nitrophenyl phosphate; D339N, aspartic acid 339 replaced by asparagine; D383N, aspartic acid 383 replaced by asparagine; C430S, cysteine 431 replaced by serine; CTA, catalytic domain of human Cdc25A; CTC, catalytic domain of human Cdc25C; Cdk, cyclin-dependent kinase; GST, glutathione *S*-transferase.

Table 1. *Kinetic data for Cdc25 wt and mutant proteins*

Enzyme	K_m (μM)	k_{cat} (min^{-1})[a]	pK_{a1}
GST-Cdc25A wt	36	0.14	5.65[b]
GST-Cdc25C wt	36	0.08	–
D339N	31	0.13	5.6[b]
D383N	84	<0.001	ND[c]
CTA	46	0.4	–
CTC	45	0.16	–
C430S	–[d]	–[d]	–
GST	–[d]	–[d]	–

[a] Enzyme concentrations 50 nM (up to 18 μM D383N) in 50 mM Tris, pH 8, 50 mM NaCl, 1 mM EDTA, and 1 mM DTT, using mFP as artificial substrate, room temperature, reaction time 1 h, except for D383N (up to 10 h).

[b] Fitted to $y = c/[(1 + H^+/K_{a1})(1 + K_{a2}/H^+)]$.

[c] ND, not determined; phosphatase activity was too low for accurate measurements.

[d] No phosphatase activity detectable.

lar & Russell, 1992). The human Cdc25C protein phosphatase dephosphorylates two inhibitory sites on the cyclin-dependent kinase (Cdk) subunit Cdc2: Thr 14 and Tyr 15; dephosphorylation of these residues activates Cdc2/cyclin B1 kinase (Dunphy & Kumagai, 1991; Gautier et al., 1991; Millar et al., 1991). This process is believed to trigger cells to enter mitosis (Russell & Nurse, 1986; Hoffmann et al., 1993). The replacement of the catalytic cysteine in the highly conserved HCEFSSER active site motif with a serine residue leads to complete inactivation of Cdc25, as is the case with other protein phosphatases (Flint et al., 1993; Davis et al., 1994; Zhou et al., 1994; Table 1). In humans, two more members of the Cdc25 family are known, Cdc25A and Cdc25B (Sadhu et al., 1990; Galaktionov & Beach, 1991; Nagata et al., 1991; Jinno et al., 1994). Their in vitro phosphatase activities are generally comparable to that of Cdc25C (Sadhu et al., 1990; Galaktionov & Beach, 1991). In vivo, however, they probably act on different Cdk complexes earlier in the cell cycle; specifically, Cdk2/cyclin E and Cdk2/cyclin A (Hoffmann et al., 1994). Human Cdc25A and Cdc25B recently have been implicated in oncogenesis, and they represent potential therapeutic targets for anticancer drugs (Galaktionov et al., 1995b).

Figure 1 shows block diagrams of the three human Cdc25 homologues. Amino acid alignments show very little similarity in the N-terminus (<30%); this is also the case for Cdc25 proteins from different species. Several N-terminal deletions of Cdc25 from different species have been reported. Nagata and others found that the C-terminal 152 residues in human Cdc25B were still capable of complementing $Cdc25^{ts}$ *Schizosaccharomyces pombe* mutants (Nagata et al., 1991). Horiguchi and co-workers reported that the C-terminal 211 residues of human Cdc25B retained activity in an assay using *p*-nitrophenyl phosphate (pNPP) (Horiguchi et al., 1994). Lee and colleagues identified residues 258–435 as a catalytically active fragment in the 473 amino acid human Cdc25C (Lee et al., 1992). Injection of protein or of an expression vector coding for the 141 amino acid C-terminal domain of the 480 amino acid *Drosophila* Cdc25 induced maturation in *Xenopus* oocytes; similar results were observed by Gautier et al. (1991) and Kumagai and Dunphy (1991). Nargi and Woodford-Thomas (1994) demonstrated that residues 185–465 of mouse Cdc25M1 were sufficient for pNPP activity as well as for the stimulation of Cdc2 kinase activity. As for C-terminal deletions, Gautier et al. (1991) and colleagues showed that deletions ΔC79, ΔC111, and ΔC204 were all completely inactive, suggesting that the C-terminus is essential for catalysis.

In this paper, we identify a likely candidate for the catalytic aspartic acid in the C-terminal catalytic domain of the Cdc25 family. Using alignments of the active site loops and the catalytic aspartic acids from a variety of protein phosphatases, as well as homology modeling techniques, we have created a three-dimensional model of the active site region of Cdc25 based on the PTP1b and *Yersinia* PTPase crystal structures (Kinemage 1). Based on a comprehensive comparison of sequences and structures of a variety of tyrosine- and dual-specificity protein phosphatases, we propose a general architecture for the phosphate binding loop and the loop containing the catalytic aspartic acid residue.

Results and discussion

The C-terminus of Cdc25 contains all residues important for catalysis

In order to directly compare kinetic parameters of N-terminal deletions with those of full-length enzymes, we expressed glutathione *S*-transferase (GST) fusion proteins of N-terminal deletions of Cdc25A (ΔN317, CTA) and Cdc25C (ΔN258, CTC), leaving 31 and 33 residues, respectively, preceding the highly conserved LIGD motif. Both mutants were active in phosphatase assays using 3-*O*-methylfluorescein phosphate (mFP) as artificial

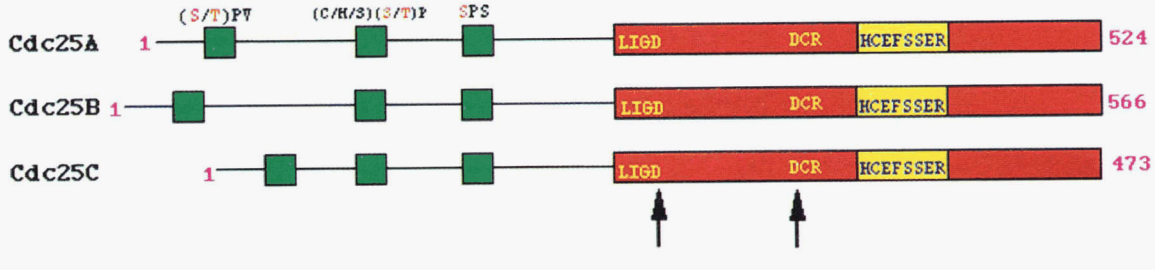

Fig. 1. Block diagram for the three human Cdc25 homologs. The catalytic domain is indicated as a red box starting with the LIGD motif. Lengths of the proteins are given by amino acid residue numbers. Conserved phosphorylation sites are shown as green boxes in the N-termini; their consensus sequences are shown above. Residues that are phosphorylated are shown in red. The positions of the two aspartic acid residues described in this paper are indicated by arrows.

substrate (Table 1) and were also capable of stimulating Cdc2/cyclin B or Cdk2/cyclin A kinase activities in kinase assays (data not shown). K_m values for mFP were found to be essentially the same in CTA and CTC as in the full-length proteins; their catalytic activity is increased 2.8- and 2-fold, respectively.

These results convincingly show that the residues essential for phosphatase activity are confined to the C-terminus of Cdc25, comprising approximately one third of the total protein. They underscore the two-domain architecture of Cdc25. The N-terminus has been proposed to serve as a regulatory domain tuning the phosphatase activity of Cdc25. It is known that the N-terminus is phosphorylated in vivo and that phosphorylation enhances Cdc25 phosphatase activity both in vitro and in vivo (Izumi et al., 1992; Kumagai & Dunphy, 1992; Hoffmann et al., 1994; Strausfeld et al., 1994; Galaktionov et al., 1995a). Figure 1 shows three conserved phosphorylation sites in the N-terminus of the three human Cdc25 homologues that have been identified in vivo for Cdc25C (Strausfeld et al., 1994).

Alignment and motifs of PTPases

In Figure 2, protein phosphatases are grouped according to their active site signatures and sequences around invariant aspartic acid residues. Five different families can be distinguished – the protein tyrosine phosphatases; the low molecular weight protein phosphatases (LMW-PPases; Mondesert et al., 1994; Zhang et al., 1994b); the Cdc25 family; Cl100, MKP-1, and Pac-1 gene products of growth-factor-inducible genes that appear to regulate MAP kinases (Keyse & Emslie, 1992; Rohan et al., 1993); and, finally, the heterogeneous group of small dual-specificity protein phosphatases.

The PTPases share a W(P/L/K)D motif approximately 30–50 amino acids upstream of the active site. From the crystal structures of PTP1b and *Yersinia* PTPase and from site-directed mutagenesis of the conserved aspartic acid residue (WP**D**) in *Yersinia* PTPase, it was proposed that this residue acts as a catalytic acid/base (Stuckey et al., 1994; Zhang et al., 1994c).

The low molecular weight protein phosphatases are structurally different from the PTPases in that the active site is located in the N-terminus rather than the C-terminus. Interestingly, a DP(W/Y) motif is conserved in the extreme C-terminus of that family. Site-directed mutagenesis of the conserved aspartic acid residue in bovine heart LMW-PTPase leads to drastically reduced catalytic activity, suggesting that this residue acts as the catalytic acid/base (Zhang et al., 1994b).

In the Cdc25 family, a highly conserved DCR motif is located 47 residues upstream of the active site – a spacing very similar to that of WPD in *Yersinia* PTPase (46 amino acids). A second highly conserved aspartic acid is located in the LIGD signature about 150 residues upstream of the active site.

It was noted previously that a DCR motif is also present in a newly found group of protein phosphatases, including human Cl100, MKP-1, and Pac-1 (Keyse & Ginsburg, 1993). However, in that family, a second conserved EDN motif is found at approximately the same sequence position as the WPD and DCR motif in the PTPase and Cdc25 families, respectively.

The last family comprises small dual-specificity protein phosphatases, such as VHR or Cdi1, that do not share either of the other motifs above (Ishibashi et al., 1992; Gyuris et al., 1993; Zhou et al., 1994). However, they all have an aspartic acid residue about 30 amino acids upstream of their active sites (Fig. 2), and D92 indeed has been identified as the catalytic acid/base in VHR protein phosphatase (Denu et al., 1995).

An essential aspartic acid residue in Cdc25

On the basis of the alignments described in Figure 2 and the fact that the Cdc25 catalytic domain is located in the C-terminus, we decided to construct the D339N (LIGD motif) and D383N (DCR motif) mutants of human Cdc25A. Both mutants were

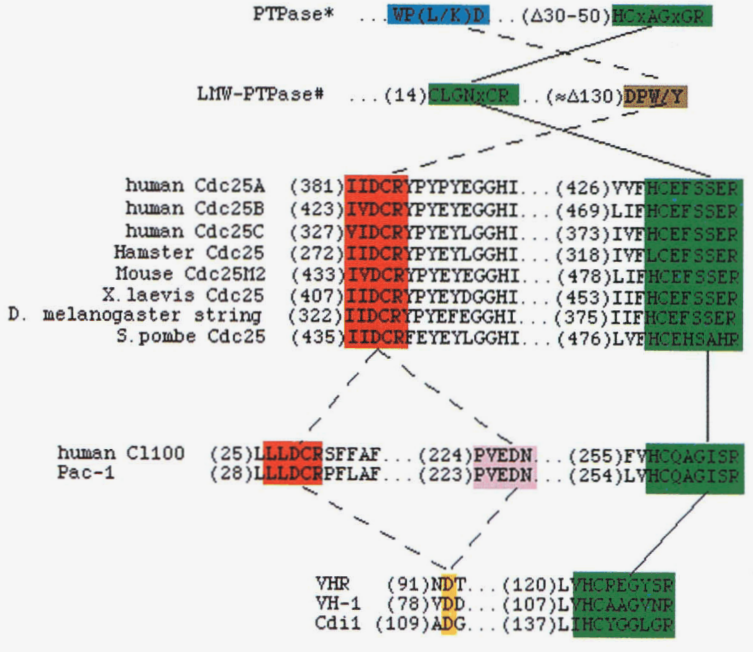

Fig. 2. Grouping of PTPases on the basis of the sequences around potential catalytic aspartic acids and the active sites in different PTPases. Active sites are highlighted in green. Amino acids are numbered from initiating methionine. Two aspartic acids are highlighted in the cases of Cl100 and Pac-1 – the N-terminal LLDCR motif is similar to the DCR motif in Cdc25, whereas the PVEDN motif has the same relative spacing as the catalytic acids in the PTPases. The motifs for PTPases and LMW-PTPases are composed from the following sequences: PTPase* – *Yersinia* PTPase (Michiels & Cornelis, 1988), yeast PTP1 and PTP2 (Guan et al., 1991), human T-cell PTP1 (Cool et al., 1989), rat PTP1 (Guan et al., 1990), human PTP1C (Shen et al., 1991), rat LAR (Streuli et al., 1988), and human PTP1b (Tonks et al., 1988); LMW-PTPase# – bovine LMW-PTPase, human LMW-PTPase, *Saccharomyces cerevisae* LMW-PTPase (Mondesert et al., 1994; Su et al., 1994; Zhang et al., 1994a).

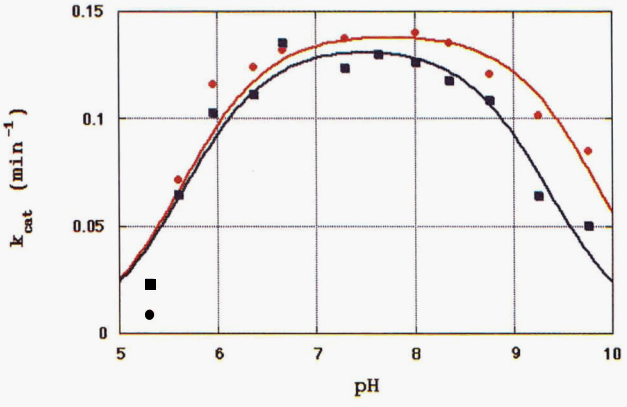

Fig. 3. pH profiles of GST-Cdc25A wild-type (red circles) and the D339N mutant protein (blue squares). Buffers used in the experiments are described in the Materials and methods section. Each data point represents the average of three measurements. Data points were fitted to $y = c/[(1 + H^+/K_{a1})(1 + K_{a2}/H^+)]$; the resulting p$K_{a1}$ values are shown in Table 1.

expressed as GST fusion proteins in *Escherichia coli*. As summarized in Table 1, the D339N mutant exhibited wild-type K_m and k_{cat} values with mFP.

Phosphatase activity was reduced at least 150-fold, and the K_m was found to be somewhat higher in the D383N mutant than in the wild-type enzyme (Table 1). In a control experiment, neither the GST-Cdc25A C430S mutant, in which the active site cysteine was replaced by a serine residue, nor GST alone showed any detectable phosphatase activity with mFP as substrate (Table 1). The pH profiles of GST-Cdc25A wt and the D339N mutant were both bell-shaped and essentially identical, exhibiting an apparent pK_{a1} of 5.6 (Fig. 3). This value is in agreement with pK_as reported for *Yersinia* PTPase and VHR (Zhang et al., 1994c; Denu et al., 1995) and falls in the range of ionizations for the side chains of aspartic acid, glutamic acid, and histidine. Unfortunately, owing to the extremely low phosphatase activity of the D383N mutant, we have not been able to determine apparent pK_a values for it. D383N was also inactive in stimulating Cdc2 kinase activity, whereas D339N retained about 65% of the wild-type activity (data not shown). These results suggest that aspartic acid 383 serves the same function as the catalytic aspartic acid in the WPD motif in PTP1b or *Yersinia* PTPase and in the NDT motif in VHR, respectively.

Secondary structure prediction and homology modeling of Cdc25 core

To determine whether there is a common structural motif that is defined by the active site and the motifs including the potential catalytic aspartic acid, we performed secondary structure predictions for PTP1b, *Yersinia* PTPase, VHR, and Cdc25. A region of approximately 50–70 amino acid residues around the catalytic aspartic acids and the active sites showed a strong correlation in secondary structure elements for the four proteins. The results of the secondary structure predictions are summarized in Figure 4A. In all cases, the catalytic aspartic acid motif is situated in a loop between a β-sheet and a long α-helix. The α-helix is followed by a loop region that includes inserts in the cases of *Yersinia* PTPase and Cdc25. The active site loop is situated between a short β-sheet and an α-helix. The secondary structure elements found in the crystal structures of *Yersinia* PTPase and PTP1b are indicated by the small letters in Figure 4A.

Fig. 4. Sequence alignment and secondary structure prediction of catalytic cores of representative PTPases, dual-specificity protein phosphatases, and Cdc25. (**A**) Secondary structure prediction for PTP1b (residues 168–226), VHR (residues 82–125), *Yersinia* PTPase (residues 345–415), and Cdc25A (residues 377–442) obtained using the PHD algorithm. B, predicted β-sheet; H, predicted α-helix; b, β-sheet found in crystal structure; h, α-helix found in crystal structure. The proposed catalytic aspartic acid residues (D, yellow) and the active site cysteines (C, pink) are printed in bold. The consensus between predicted secondary structure and secondary structure elements found in crystal structures is highlighted in blue (β-sheet) and in red (α-helix). (**B**) Secondary structure elements found in the crystal structure of bovine LMW-PTPase (residues 123–157 and 1–23). (**C**) Secondary structure prediction for Cdi1 PTPase (residues 100–151). The question mark indicates the proposed catalytic aspartic acid residue.

Fig. 5. Ribbon diagram of the Cdc25 structural model. Active site loop residues HCEFSSER are labeled; the proposed catalytic acid D383 is shown in balls and sticks. The distance between the sulphur atom of the active site cysteine and Cα of the catalytic acid D is ≈12 Å.

Fig. 6. Superposition of the core regions of PTP1b (residues 168–226; pink), *Yersinia* PTPase (residues 345–415; blue), and the Cdc25 model (residues 377–442; yellow). Regions in the Cdc25 model outside secondary structure correlations are shown in gray.

The minimal common structural elements (highlighted in Fig. 4) were used for homology modeling of a Cdc25 core region. The resulting structure is shown in Figure 5 (Kinemage 1). The crystal structures of corresponding regions of PTP1b and *Yersinia* PTPase were superimposed onto the model (Fig. 6). The three structures render a minimal core and share the same basic geometry. The active site loops are very similar in all three structures, with the nucleophilic cysteinyl residue in the center of the loop. None of the side chains of the residues between the cysteine and the arginine point into the phosphate binding site. The position of the histidine residue preceding the cysteine seems to allow hydrogen bonding to the backbone carbonyl of the cysteine. This hydrogen bond has also been observed in the crystal structures of *Yersinia* PTPase and PTP1b. *Yersinia* PTPase mutant proteins in which the highly conserved histidine was replaced by asparagine or alanine retained about 1.2 and 0.03%, respectively, of wild-type catalytic activity. Furthermore, the pK_a of the active site cysteine was significantly altered in both cases (Zhang & Dixon, 1993). These data suggest that the hydrogen bond between the active site histidine and cysteine residues participates in the stabilization of the active site thiolate.

In all three structures, the loops containing the catalytic aspartic acids are situated about 10 Å away from the active site cysteines. The most prominent feature of the three structures beside the active site loop is the long α-helix following the loop containing the catalytic aspartic acid. The loop region following this helix allows for insertions without changing the position of the active site loop relative to the aspartic acid (Fig. 6). In the crystal structures of PTP1b (E115) and *Yersinia* PTPase (E290), glutamate residues orient the active site arginines through hydrogen bonding. In our Cdc25 model, a highly conserved glutamate residue (HCEXXXXR) located *in* the active site loop is in hydrogen bonding distance of the active-site arginine (Fig. 6). Although the homology model does not allow conclusions regarding side-chain interactions owing to the fact that residues outside the core regions were left out, one may speculate that this active site glutamate residue plays a role similar to that of E290 in *Yersinia* PTPase and E115 in PTP1b. Site-directed mutagenesis experiments are under way to test this hypothesis.

Structure comparison of PTPases and LMW-PPases

The three-dimensional structures of two LMW-PPases have been solved to date (Logan et al., 1994; Su et al., 1994; Zhang et al., 1994a). In Figure 7, we superimposed the crystal structure of bovine heart LMW-PPase (Brookhaven Protein Data Bank entry 1PNT) on the core regions from the crystal structures of PTP1b and *Yersinia* PTPase. Even though the positions in the amino acid sequence of the LMW-PPase active site and the DP(W/Y) motif containing the catalytic acid are very different than in the other protein phosphatases, the basic geometry of the active site and of the loop containing the aspartic acid is essentially the same. The minimal core structure is assembled from the two ends of the protein, leading to the superposition of the aspartic acids in the DP(W/Y) motif and the WPD motif in PTP1b and *Yersinia* PTPase, respectively. The secondary structure elements are also comparable (Fig. 4B), in that the aspartic acid loop and the active site motif are both located be-

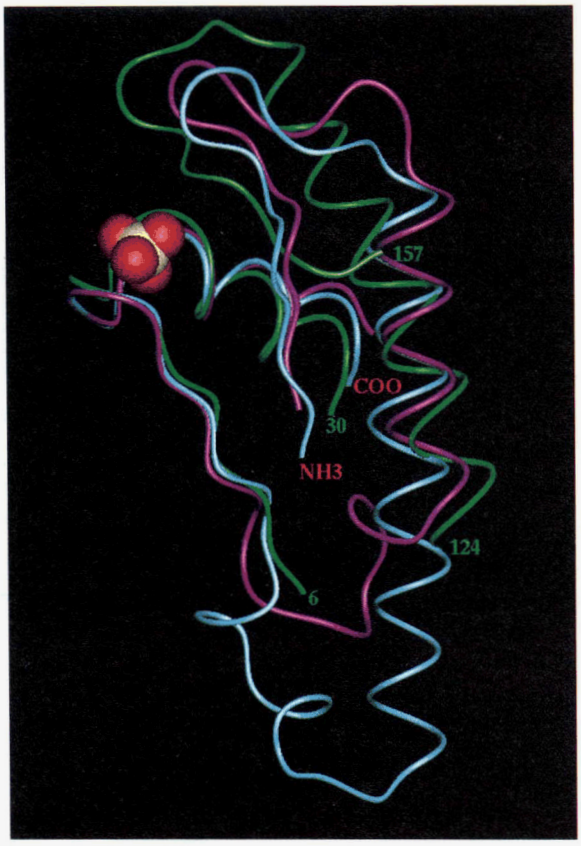

Fig. 7. Superposition of the core regions of PTP1b (residues 168–226; pink), *Yersinia* PTPase (residues 345–415; blue), and bovine LMW-PTPase (green). The core region of LMW-PTPase is assembled from the N-terminus (residues 6–34, active site) and the C-terminus (residues 124–157). Note that the direction of the sequence around the long helix and the catalytic acid loop (residues 124–157) is reversed. For better visualization of the active site loop, a phosphate group was modeled into the active site of *Yersinia* PTPase by superimposing tungstate in the crystal structure with a phosphate group.

tween a β-sheet and an α-helix. The common three-dimensional geometry of the active site of these phosphatases is very intriguing in light of the low amino acid sequence similarity. It will be interesting to see if future protein phosphatase structures share the same architecture.

Prediction of the catalytic aspartic acid residue in other protein phosphatases

The common three-dimensional model described above might be helpful in the identification of the catalytic aspartic acid residue in other protein phosphatases. Figure 4C shows the secondary structure prediction for Cdi1, a protein phosphatase that associates with Cdk2 (Gyuris et al., 1993). From this alignment, one would predict that D110 serves as the catalytic aspartic acid residue in Cdi1.

Conclusion

We have identified D383 as the potential catalytic acid in the C-terminus of Cdc25 protein phosphatase. Our studies are consistent with a two-domain architecture of Cdc25 consisting of a distinct catalytic C-terminal domain and a regulatory N-terminal domain. Using sequence alignments and secondary structure prediction, we were able to build a homology model of a 70 amino acid segment of Cdc25 around the active site and D383, illustrating the remarkable structural similarity of protein phosphatases. The architecture of this core region accommodates significant sequence variability and/or insertions and deletions. In the case of the low molecular weight protein phosphatases, even permutations are possible in this core region without changing the basic architecture. Stone and Dixon proposed in their recent review that, "in light of the overall lack of sequence identity, the structural and mechanistic similarities between PTPases may well represent an example of convergent evolution" (Stone & Dixon, 1994).

An important unresolved question is the substrate specificity of protein phosphatases. Although the architecture of the active site and the basic chemical mechanism of protein phosphatases are intriguingly similar, these enzymes exhibit very different substrate specificities. Whereas PTP1b accepts peptidic tyrosyl phosphate substrates, VHR is able to dephosphorylate both threonyl and tyrosyl phosphates in peptides. Both of these enzymes were tested with artificial, customized peptides, primarily because of the lack of knowledge regarding their physiological substrates. Cdc25, on the other hand, hardly accepts any substrate other than its physiological ones, the Cdk/cyclin complexes. One can imagine that the ability to distinguish between phosphotyrosine and phosphothreonine residues can be achieved by variation in the depth of the phosphate binding pocket and in the residues lining this pocket. The mechanism for the recognition of the more complex, native substrates, on the other hand, might involve residues outside the active site, including, perhaps, the N-terminal extensions present in Cdc25.

Materials and methods

Cloning of mutants and site-directed mutagenesis

The Cdc25A aspartic acid to asparagine mutants at positions 339 and 383 were cloned by PCR site-directed mutagenesis. A mutant fragment bearing the D339N substitution was generated by PCR using the primers (5′-CATCATGGGACCTTATAGGAAACTTC TCCAAGGG-3′) and (5′-GTAGTACCCTGGAGAGAGTCTTC TTTTGAGCGTC-3′). Following *Ppu*MI digestion, the mutant fragment was swapped for the *Ppu*MI internal fragment (bp 1005–1312) of the wild-type *pGEXcdc25A* clone. A mutant fragment bearing the D383N substitution was generated using primers (5′-CATCATCCATGGAACTGGGCCCGAGCCCCGC-3′) and (5′-GTAGTAGTATACCCATAGCTGTCAACTACTATTG-3′). This fragment replaced the wild-type *Nco*I–*Nde*I fragment (bp 1–1164) from *pGEXcdc25A*. The Cdc25A C430S mutant construct was made by generating two overlapping fragments (N-terminal and C-terminal) bearing the mutation in separate primary PCR reactions and combining them in a second reaction using the distal primers. The N-terminal fragment was produced using (5′-CATCA TCCATGGAACTGGGCCCGAGCCCCGC-3′) and (5′-AGAAG AAAACTCGGAGTGAAACACAAC-3′). The C-terminal fragment was made using (5′-GTTGTGTTTCACTCCGAGTTTTCT TCT-3′) and (5′-GCCAAGCTTAGAGCTTCTTCAGACG-3′). The primary PCR products were then combined as the template in the secondary PCR reaction using primers (5′-CATCATCCATG

GAACTGGGCCCGAGCCCCGC-3′) and (5′-GCCAAGCTTAG AGCTTCTTCAGACG-3′) to yield a full-length product that was cloned into *pGEX* as an *NcoI/Hin*dIII fragment. *CTA* is a truncated, double-tagged construct of the C-terminal portion of *Cdc25A* from bp 966 to 1586. It was constructed by PCR amplification using the primers (5′-CATCATGAATTCTGGCATC TTCCCCCAAAGGAACC-3′) and (5′-CATCATAAGCTTCA ATGATGATGATGATGATGGAGCTTCTTCAGACGACTG TACATCTCCC-3′). The resulting PCR fragment contains six His that were added at the C-terminus as an affinity tag. The fragment was cloned into a *pGEX* vector, replacing the existing *Eco*RI/*Hin*dIII fragment. *CTC* was constructed by *Xba*I and *Hin*dIII digestion of *pGEX* and the C-terminus of *cdc25C* from bp 651 to 1646 followed by PCR using the primers (5′-GATC AGGTGGTGGTGGCGGCCGTTTGGTACCTCGAG-3′) and (5′-GATCCTCGAGGTACCAAACGGCCGCCACCACCA CT-3′). Six His were added at the C-terminus as an affinity tag by PCR amplification of bp 1121–1646 using primers (5′-CATC ATAGATCTGAAGTATGTCAACCC-3′) and (5′-CATCATAA GCTTAATGATGATGATGATGATGGGCGGCTGGGCTCA TGTCCTTCACC-3′). The His-tag fragment was cloned into *CTC* by replacing the existing *Bgl*II/*Hin*dIII fragment with the His-tag fragment. Both constructs have thrombin cleavage sites just upstream of the *Cdc25* C-terminus coding sequences, adding 12 and 16 extra amino acid residues to the N-terminus of CTA and CTC, respectively. All mutations were confirmed by sequencing.

Enzyme purifications

GST fusion proteins were purified as described previously (Galaktionov & Beach, 1991).

Phosphatase assays

Cdc25 phosphatase activity was measured using the fluorogenic mFP (USB, Cat.# 19060) as artificial substrate in 50 mM Tris, pH 8, 50 mM NaCl, 1 mM EDTA, and 1 mM DTT. Cdc25 stock solutions were preincubated in 10 mM DTT for 15 min on ice and then diluted accordingly into assay buffer to a final concentration of 1 mM DTT. Fluorescence was monitored on a Biosearch Cytofluor II fluorescence reader at room temperature over a time period ranging from 1 to 10 h.

Kinase assays

Stimulation of Cdk activity by Cdc25 was measured as described (Pines & Hunter, 1989; Pagano et al., 1992) using Cdc2/cyclin B or Cdk2/cyclin A immunoprecipitates from hydroxyurea-blocked HeLa cells.

pH profiles

The following buffers were used: pH 4–5.6, 100 mM acetate; pH 5.8–6.5, 50 mM succinate; pH 6.6–7.3, 50 mM 3,3-dimethylglutarate; pH 7.5–8.4, 100 mM glycinamide; pH 9–10.5, 100 mM glycine-NaOH. Buffers were adjusted to the same conductivity of 25 mS/cm with 5 M NaCl; 1 mM EDTA and 1 mM DTT were present in all buffers. Experimental data were analyzed using the KinetAsyst software package.

Sequence alignments

Sequences were aligned manually or using the Clustal algorithm in the DNAStar/MegAlign software package.

Structure predictions

The PHD algorithm (Rost & Sander, 1993) was used for the prediction of the secondary structure elements

Homology model of Cdc25

Three-dimensional coordinates of the protein backbone rendering the residues shown in Figure 4A from the structure of *Yersinia* PTPase were used for homology modeling of human Cdc25. Human Cdc25A, B, and C share a high degree of similarity in this region (>65%). Modeling was performed with the Protein Workbench software package in Quanta from MSI. The amino acid sequences of human Cdc25C and *Yersinia* PTPase were first aligned manually to match the active site residues and the catalytic aspartic acids. The coordinates of the backbone nonhydrogen atoms of *Yersinia* PTPase that matched the secondary structure prediction for Cdc25 were then copied onto Cdc25; side-chain coordinates were ignored at that point. Missing coordinates were generated using the regularization algorithm in Quanta. The resulting Cdc25 structure was energy minimized using 200 steps of the steepest descent algorithm, followed by 5000 steps of the adopted-base Newton Raphson (ABNR) algorithm. All atoms, including polar hydrogens, and all side chains were allowed to move freely. In the next step the structure was heated up to 1,000 K using 3,000 steps or a total time of 3 ps. After heating, the system was allowed to equilibrate for 5 ps (5,000 steps). Formal charges were turned off in all dynamic simulations. Finally, the system was subjected to simulated annealing from 1,000 K to 300 K and then energy minimized with formal charges turned on.

Acknowledgments

We thank Mark Saper and David Barford for making the coordinates of the *Yersinia* PTPase and PTP1b available to us. We thank Muz Mansuri and Giulio Draetta for critical reading of the manuscript and Jack Dixon and Xu Xu for stimulating discussions.

References

Barford D, Flint AJ, Tonks NK. 1994. Crystal structure of human protein tyrosine phosphatase 1B. *Science 263*:1397–1404.

Cho H, Ramer SE, Itoh M, Kitas E, Bannwarth W, Burn P, Saito H, Walsh CT. 1992. Catalytic domains of the LAR and CD45 protein tyrosine phosphatases from *Escherichia coli* expression systems: Purification and characterization for specificity and mechanism. *Biochemistry 31*:133–138.

Cool DE, Tonks NK, Charbonneau H, Walsh KA, Fischer EH, Krebs EG. 1989. cDNA isolated from a human T-cell library encodes a member of the protein-tyrosinephosphatase family. *Proc Natl Acad Sci USA 86*: 5257–5261.

Davis JP, Zhou MM, Van Etten RL. 1994. Kinetic and site-directed mutagenesis studies of the cysteine residues of bovine low molecular weight phosphotyrosyl protein phosphatase. *J Biol Chem 269*:8734–8740.

Denu JM, Zhou G, Guo Y, Dixon JE. 1995. The catalytic role of aspartic acid-92 in a human dual-specific protein-tyrosine phosphatase. *Biochemistry 34*:3396–3403.

Dunphy WG, Kumagai A. 1991. The cdc25 protein contains an intrinsic phosphatase activity. *Cell 67*:189–196.

Fischer EH, Charbonneau H, Tonks NK. 1991. Protein tyrosine phosphatases: A diverse family of intracellular and transmembrane enzymes. *Science 253*:401–406.

Flint AJ, Gebbink MF, Franza Jr BR, Hill DE, Tonks NK. 1993. Multi-site phosphorylation of the protein tyrosine phosphatase, PTP1B: Identification of cell cycle regulated and phorbol ester stimulated sites of phosphorylation. *EMBO J 12*:1937–1946.

Galaktionov K, Beach D. 1991. Specific activation of cdc25 tyrosine phosphatases by B-type cyclins: Evidence for multiple roles of mitotic cyclins. *Cell 67*:1181–1194.

Galaktionov K, Jessus C, Beach B. 1995a. Raf1 interaction with Cdc25 phosphatase ties mitogenic signal transduction to cell cycle activation. *Genes Dev 9*:1046–1058.

Galaktionov K, Lee A, Eckstein JW, Draetta G, Meckler J, Loda M, Beach D. 1995b. Cdc25 phosphatases as potential human oncogenes. *Science 269*:1575–1577.

Gautier J, Solomon MJ, Booher RN, Bazan JF, Kirschner MW. 1991. Cdc25 is a specific tyrosine phosphatase that directly activates p34cdc2. *Cell 67*: 197–211.

Guan KL, Deschenes RJ, Qiu H, Dixon JE. 1991. Cloning and expression of a yeast protein tyrosine phosphatase. *J Biol Chem 266*:12964–12970.

Guan KL, Dixon JE. 1990. Protein tyrosine phosphatase activity of an essential virulence determinant in *Yersinia*. *Science 249*:553–556.

Guan KL, Huan RS, Watson SJ, Geahlen RL, Dixon JE. 1990. Cloning and expression of a protein-tyrosine phosphatase. *Proc Natl Acad Sci USA 87*:1501–1505.

Gyuris J, Golemis E, Chertkov H, Brent R. 1993. Cdi1, a human G1 and S phase protein phosphatase that associates with Cdk2. *Cell 75*:791–803.

Hoffmann I, Clarke PR, Marcote MJ, Karsenti E, Draetta G. 1993. Phosphorylation and activation of human cdc25-C by cdc2-cyclin B and its involvement in the self-amplification of MPF at mitosis. *EMBO J 12*: 53–63.

Hoffmann I, Draetta G, Karsenti E. 1994. Activation of the phosphatase activity of human cdc25A by a cdk2-cyclin E dependent phosphorylation at the G1/S transition. *EMBO J 13*:4302–4310.

Horiguchi T, Nishi K, Hakoda S, Tanida S, Nagata A, Okayama H. 1994. Dnacin A1 and Dnacin B1 are antitumor antibiotics that inhibit Cdc25 phosphatase activity. *Biochem Pharmacol 48*:2139–2141.

Ishibashi T, Bottaro DP, Chan A, Miki T, Aaronson SA. 1992. Expression cloning of a human dual-specificity phosphatase. *Proc Natl Acad Sci USA 89*:12170–12174.

Izumi T, Walker DH, Maller JL. 1992. Periodic changes in phosphorylation of the *Xenopus* cdc25 phosphatase regulate its activity. *Mol Biol Cell 3*: 927–939.

Jinno S, Suto K, Nagata A, Igarashi M, Kanaoka Y, Nojima H, Okayama H. 1994. Cdc25A is a novel phosphatase functioning early in the cell cycle. *EMBO J 13*:1549–1556.

Keyse SM, Emslie EA. 1992. Oxidative stress and heat shock induces a human gene encoding a protein-tyrosine phosphatase. *Nature 359*:644–646.

Keyse SM, Ginsburg M. 1993. Amino acid sequence similarity between Cl100, a dual-specificity MAP kinase phosphatase, and Cdc25. Trends in Biochemistry. *Science 18*:377–378.

Kumagai A, Dunphy WG. 1991. The cdc25 protein controls tyrosine dephosphorylation of the cdc2 protein in a cell-free system. *Cell 64*:903–914.

Kumagai A, Dunphy WG. 1992. Regulation of the cdc25 protein during the cell cycle in *Xenopus* extracts. *Cell 70*:139–151.

Lee MS, Ogg S, Xu M, Parker LL, Donoghue DJ, Maller JL, Piwnica-Worms H. 1992. cdc25+ encodes a protein phosphatase that dephosphorylates p34cdc2. *Mol Biol Cell 3*:73–84.

Logan TM, Zhou MM, Nettesheim DG, Meadows RP, Van Etten RL, Fesik SW. 1994. Solution structure of a low molecular weight protein tyrosine phosphatase. *Biochemistry 33*:11087–11096.

Michiels T, Cornelis G. 1988. Nucleotide sequence and transcription analysis of yop51 from *Yersinia enterocolitica* W22703. *Microb Pathol 5*:449–459.

Millar JB, McGowan CH, Lenaers G, Jones R, Russell P. 1991. p80cdc25 mitotic inducer is the tyrosine phosphatase that activates p34cdc2 kinase in fission yeast. *EMBO J 10*:4301–4309.

Millar JB, Russell P. 1992. The cdc25 M-phase inducer: An unconventional protein phosphatase. *Cell 68*:407–410.

Mondesert O, Moreno S, Russell P. 1994. Low molecular weight protein-tyrosine phosphatases are highly conserved between fission yeast and man. *J Biol Chem 269*:27996–27999.

Nagata A, Igarashi M, Jinno S, Suto K, Okayama H. 1991. An additional homolg of the fission yeast cdc25$^+$ gene occurs in humans and is highly expressed in some cancer cells. *New Biologist 3*:959–968.

Nargi JL, Woodford-Thomas TA. 1994. Cloning and characterization of a cdc25 phosphatase from mouse lymphocytes. *Immunogenetics 39*:99–108.

Pagano M, Pepperkok R, Verde F, Ansorge W, Draetta G. 1992. Cyclin A is required at two points in the human cell cycle. *EMBO J 11*:9761–9771.

Pines J, Hunter T. 1989. Isolation of a human cyclin cDNA: Evidence for cyclin mRNA and protein regulation in the cell cycle and for interaction with p34cdc2. *Cell 58*:833–846.

Pot DA, Dixon JE. 1992. Active site labeling of a receptor-like protein tyrosine phosphatase. *J Biol Chem 267*:140–143.

Rohan PJ, Davis P, Moskaluk CA, Kearns M, Krutzsch H, Siebenlist U, Kelly K. 1993. PAC-1: A mitogen-induced nuclear protein tyrosine phosphatase. *Science 259*:1763–1766.

Rost B, Sander C. 1993. Improved prediction of protein secondary structure by use of sequence profiles and neural networks. *Proc Natl Acad Sci USA 90*:7558–7562.

Russell P, Nurse P. 1986. cdc25+ functions as an inducer in the mitotic control of fission yeast. *Cell 45*:145–53.

Sadhu K, Reed SI, Richardson H, Russell P. 1990. Human homolog of fission yeast cdc25 mitotic inducer is predominantly expressed in G2. *Proc Natl Acad Sci USA 87*:5139–5143.

Schubert HL, Fauman EB, Stuckey JA, Dixon JE, Saper MA. 1995. A ligand-induced conformational change in the *Yersinia* protein tyrosine phosphatase. *Protein Sci 4*:1904–1913.

Shen SH, Bastien L, Posner BI, Chretien P. 1991. A protein-tyrosine phosphatase with sequence similarity to the SH2 domain of the protein-tyrosine kinases. *Nature 352*:736–739.

Stone RL, Dixon JE. 1994. Protein-tyrosine phosphatases. *J Biol Chem 269*: 31323–31326.

Strausfeld U, Fernandez A, Capony JP, Girard F, Lautredou N, Derancourt J, Labbe JC, Lamb NJ. 1994. Activation of p34cdc2 protein kinase by microinjection of human cdc25C into mammalian cells. Requirement for prior phosphorylation of cdc25C by p34cdc2 on sites phosphorylated at mitosis. *J Biol Chem 269*:5989–6000.

Streuli M, Krueger NX, Hall RL, Schlossman SF, Saito H. 1988. A new member of the immunoglobulin superfamily that has a cytoplasmic region homologous to the leukocyte common antigen. *J Exp Med 168*:1523–1530.

Streuli M, Krueger NX, Thai T, Tang M, Saito H. 1990. Distinct functional roles of the two intracellular phosphatase like domains of the receptor-linked protein tyrosine phosphatases LCA and LAR. *EMBO J 9*:2399–2407.

Stuckey JE, Schubert HL, Fauman EB, Zhang ZY, Dixon JE, Saper MA. 1994. Crystal structure of *Yersinia* protein tyrosine phosphatase at 2.5 Å and the complex with tungstate. *Nature 370*:571–575.

Su XD, Taddel N, Stefani M, Ramponi G, Nordlund P. 1994. The crystal structure of a low-molecular-weight phosphotyrosine protein phosphatase. *Nature 370*:575–578.

Tonks NK, Diltz CD, Fischer EH. 1988. Characterization of the major protein-tyrosine-phosphatases of human placenta. *J Biol Chem 263*:6731–6737.

Zhang M, Van Etten RL, Stauffacher CV. 1994a. Crystal structure of bovine heart phosphotyrosyl phosphatase at 2.2 Å resolution. *Biochemistry 33*:11097–11105.

Zhang Z, Harms E, Van Etten RL. 1994b. Asp 129 of low molecular weight protein tyrosine phosphatase is involved in leaving group protonation. *J Biol Chem 269*:25947–25950.

Zhang ZY, Dixon JE. 1993. Active site labeling of the *Yersinia* protein tyrosine phosphatase: The determination of the pK_a of the active site cysteine and the function of the conserved histidine 402. *Biochemistry 32*: 9340–9345.

Zhang ZY, Wang Y, Dixon JE. 1994c. Dissecting the catalytic mechanism of protein-tyrosine phosphatases. *Proc Natl Acad Sci USA 91*:1624–1627.

Zhou G, Denu JM, Wu L, Dixon JE. 1994. The catalytic role of Cys124 in the dual-specificity phosphatase VHR. *J Biol Chem 269*:28084–28090.